Engineering Oral and Parenteral Amorphous Amphotericin B Formulations against Experimental *Trypanosoma cruzi* Infections

Miriam Rolón[a,±], Dolores R. Serrano[b,c,±], Aikaterini Lalatsa[d,*], Esther de Pablo[b], Juan Jose Torrado[b,c], Maria Paloma Ballesteros[b,c], Anne Marie Healy[e], Celeste Vega[a], Cathia Coronel[a], Francisco Bolás-Fernández[f], Maria Auxiliadora Dea-Ayuela[g,*]

[a]Centro para el Desarrollo de la Investigación Científica (CEDIC), Manduvirá 635 entre 15 de Agosto y O'Leary, 1255-Asuncion, Paraguay.

[b]Departamento de Farmacia y Tecnología Farmacéutica, Facultad de Farmacia, Universidad Complutense de Madrid, Plaza Ramón y Cajal s/n, 28040-Madrid, Spain.

[c]Instituto Universitario de Farmacia Industrial (IUFI), School of Pharmacy, University Complutense, Avenida Complutense, 28040 Madrid, Spain.

[d]School of Pharmacy and Biomedical Sciences, University of Portsmouth, St. Michael's Building, White Swan Road, Portsmouth PO1 2DT, UK.

[e]School of Pharmacy and Pharmaceutical Sciences, Trinity College Dublin, Dublin 2, Ireland.

[f]Departamento de Parasitología, Facultad de Farmacia, Universidad Complutense de Madrid, Plaza Ramón y Cajal s/n, 28040-Madrid, Spain.

[g]Departamento de Farmacia, Facultad de Ciencias de la Salud, Universidad CEU Cardenal Herrera, Edificio Seminario s/n, 46113-Moncada, Valencia, Spain.

[±] Shared first co-authorship

***Corresponding authors:**

Dr. Aikaterini Lalatsa
School of Pharmacy and Biomedical Sciences
University of Portsmouth, St. Michael's Building
White Swan Road, Portsmouth PO1 2DT, UK.
Email: katerina.lalatsa@port.ac.uk
Tel: +44 023 9284 3929

Dr. María Auxiliadora Dea-Ayuela
Departamento de Farmacia, Facultad de Ciencias de la Salud, Universidad CEU Cardenal Herrera, Edificio Seminario s/n, 46113-Moncada, Valencia, Spain.
Email: mdea@uch.ceu.es
Tel: +34 961 369 000; Fax: +34 961 395 272.

This is a peer-reviewed, accepted author manuscript of the following article: Rolón, M., Serrano, D. R., Lalatsa, A., De Pablo, E., Torrado, J. J., Ballesteros, M. P., Healy, A. M., Vega, C., Coronel, C., Bolás-Fernández, F., & Dea-Ayuela, M. A. (2017). Engineering oral and parenteral amorphous amphotericin B formulations against experimental Trypanosoma cruzi infections. Molecular Pharmaceutics, 14(4), 1095-1106. https://doi.org/10.1021/acs.molpharmaceut.6b01034

Abstract

Chagas disease (CD) is a parasitic zoonosis endemic in most mainland countries of Central and South America affecting nearly 10 million people, with 100 million people at high risk of contracting the disease. Treatment is only effective if received at the early stages of the disease. Only two drugs (benznidazole and nifurtimox) have so far been marketed and both share various limitations such as variable efficacy, many side effects and long duration of treatment, thus reducing compliance. The *in vitro* and *in vivo* efficacy of poly-aggregated amphotericin B (AmB), encapsulated poly-aggregated AmB in albumin microspheres (AmB-AME) and dimeric AmB - sodium deoxycholate micelles (AmB-NaDC) was evaluated. Dimeric AmB-NaDC exhibited a promising selectivity index (SI = 3164) against amastigotes, which was much higher than those obtained for licensed drugs (benznidazole and nifurtimox). AmB-AME, but not AmB-NaDC, significantly reduced the parasitaemia levels (3.6-fold) in comparison to the control group after parenteral administration at day 7 post-infection. However, the oral administration of AmB-NaDC (10-15 mg/kg/day for 10 days) resulted in a 75 % reduction of parasitaemia levels-and prolonged the survival rate in 100% of the tested animals. Thus, the results presented here illustrate for the first time the oral efficacy of AmB in the treatment of trypanosomiasis. AmB-NaDC is an easily scalable, affordable formulation prepared from GRAS excipients, enabling treatment access worldwide and therefore it can be regarded as a promising therapy for trypanosomiasis.

Keywords: amphotericin B, albumin microspheres, oral delivery, *Trypanosoma cruzi*, sodium deoxycholate micelles.

1. Introduction

Chagas disease (CD), also known as American trypanosomiasis, is a chronic life-threatening parasitic infection caused by *Trypanosoma cruzi* that is endemic in the majority of Central and South America countries. CD affects more than 10 million people while placing approximately 100 million people at risk [1]. CD presents in two phases. An initial acute phase lasts for about 2 months after infection during which time a high number of parasites circulate in the blood with limited or no symptoms. Even decades after primary infection, parasites reside mainly in the heart and digestive musculature resulting in cardiac disorders and digestive disorders (enlargement of oesophagus or colon) in 30% and 10% of patients respectively as well as neurological symptoms. Progressive destruction of the heart muscle or the nervous system can lead to heart failure and sudden death [1].

Treating the parasitic infection in its acute phase (where the parasites reside within the blood) is of paramount importance and treatment involves benznidazole (BNZ) and nifurtimox (NFX, licensed only in Argentina and Germany). Both medicines are almost 100% effective in curing the disease if given at the onset of the acute phase. However, the efficacy of both drugs diminishes the longer a person has been infected [1]. Available treatments are far from ideal as their use is limited by: i) long duration of treatment (30, 60 or 90 days) [2], ii) variable efficacy due to naturally resistant *T. cruzi* strains [3] and iii) serious undesirable side effects (occurring in 40% of treated patients) [1] combined with contraindications for their use in pregnancy, renal or hepatic failure [4]. Ideally new chemical entities (NCEs) are required with enhanced potency, specificity, and lack of toxicity in order to provide breakthrough therapeutic benefits within a wide safety margin. However, the development of NCEs is a riskier and more expensive option [3] than repurposing or reformulating existing drugs, or combining them in novel fixed-dose combinations with enhanced efficacy and reduced duration of treatment.

Amphotericin B (AmB) is a macrolide polyene chemotherapeutic that exists in three different aggregation states: monomer, dimer and poly-aggregate, which have exhibited different safety profiles [5]. Parenteral AmB formulations, either the original micellar formulation with sodium deoxycholate (Fungizone®) or the less nephrotoxic and haemolytic liposomal formulation (AmBisome®), have been used as effective treatments for visceral leishmaniasis (VL) [6]. Current research has indicated that poly-aggregated

AmB formulations reduce the toxicity and enhance the efficacy after intravenous administration [7] compared to AmBisome® due to the larger volume of distribution [8]. However, although the activity of AmB in *T. cruzi* infections was first reported in 1960 [9] and there are several studies illustrating the *in vitro* nanomolar trypanocidal activity for Fungizone® and lipidic AmB formulations (Amphocil® and AmBisome®) [10], only a few reports describe AmBisome's *in vivo* effects in *T. cruzi* infected mice [3, 11] and there are no licensed AmB formulation in the market. However, when used against *T. cruzi* high parenteral doses (> 25mg/kg) over a prolonged duration were needed. AmB is a BCS Class IV drug with low solubility and low permeability across the gastrointestinal epithelium resulting in low oral bioavailability (< 0.9%) [12]. Although oral formulations of AmB are under research for VL [6b, 13], no reports are available for the treatment of CD *in vivo*, even though an oral AmB treatment alone or in combination with existing drugs could enhance efficacy of current treatment options avoiding AmB systemic toxicity [12a, 14].

The hypothesis underpinning this work is that amorphous dimeric AmB will be ideal for CD treatment via the oral route, as it maintains high activity and enhanced solubility in aqueous media providing greater oral bioavailability. In contrast, parenteral poly-aggregated formulations of AmB with a higher volume of distribution will allow for accumulation of AmB in tissues in the acute phase preventing parasite migration and reducing the parasitic load in the chronic phase of CD. Thus, we have entrapped AmB in the polyaggregate state within albumin microspheres (AmB-AME) and prepared lyophilized amorphous micellar sodium deoxycholate AmB dispersions (AmB-NaDC). The proposed formulations allow for a higher dose to be administered with longer dosing intervals, as evidenced by the presented *in vitro* and *in vivo* efficacy studies against *T. cruzi* in BALB/c mice, and can be up-scaled resulting in cost-effective parenteral and oral solutions for *T. cruzi* treatment.

2. Materials and methods

2.1. Materials.

Amphotericin B (>95% HPLC) was obtained from Azelis (Barcelona, Spain). Serum albumin solution (20%) was obtained from Instituto Grifols SA (Barcelona, Spain). All chemicals, solvents and acids, unless otherwise stated, were of ACS grade or above and were obtained from Sigma-Aldrich (Madrid, Spain) or Panreac S.A. (Barcelona, Spain)

and used without further purification. Cell culture media were bought from Sigma-Aldrich (Madrid, Spain).

2.2. Preparation of AmB formulations

A summary of all formulations is illustrated in Table S1 in Supplementary material.

Dimeric AmB

Before adding AmB (50 mg) into the aqueous solution containing 41 mg of NaDC, the pH was adjusted to 12.0 using 2 M sodium hydroxide. The mixture was stirred until a clear orange solution was obtained, when the pH was reduced to 7.4 ± 0.05 by adding 2 N ortho-phosphoric acid. The dimeric micellar sodium deoxycholate AmB formulation (AmB-NaDC) was frozen at - 40°C and lyophilized (Telstar, Barcelona, Spain) [5].

Poly-aggregated AmB

AmB (50 mg) was added in 10 ml of an aqueous solution containing 41 mg of sodium deoxycholate (NaDC, Fluka Chemie A. G., Buchs, Switzerland), 10 mg of dibasic sodium phosphate and 0.9 mg of monobasic sodium phosphate (Panreac S.A., Barcelona, Spain). The dispersion was stirred until a homogeneous yellow suspension was obtained (5 mg mL^{-1}, pH 7). The resultant suspension was frozen at - 40°C and lyophilized (Telstar, Barcelona, Spain) for 48 h [15].

Microencapsulated poly-aggregated AmB

Amphotericin B within albumin microspheres (AmB-AME) was prepared as previously described [8] with some modifications. Briefly, poly-aggregated AmB suspension (213 ml) was mixed with 100 ml of a 20% serum albumin solution (Instituto Grifols SA, Barcelona, Spain). The mixture was spray dried in the open mode using a Büchi B 191 spray dyer (Flawil, Switzerland) fitted with a standard 0.7 mm 2-fluid nozzle. The following parameters were used for spray-drying: an air flow rate of 463 L h^{-1}, a 120 °C inlet temperature, a pump rate of 3 mL min^{-1} and 100% aspiration. The resulting outlet temperature was set between 70-75°C. The encapsulation efficiency of AmB into albumin microspheres was quantified as previously described [15]. Unloaded albumin microspheres (AME) were also prepared under the same conditions and starting materials but without including the poly-aggregated AmB suspension.

Physical mixtures

AmB and all other excipients used in the preparation of dimeric AmB-NaDC or AmB-AME were mixed using a mortar and pestle in the same ratio as in the final formulations.

2.3. Characterization of AmB formulations

AmB aggregation state, particle size and water sorption kinetic profiles were measured [8]. Poly-aggregated AmB, poly-aggregated AmB-AME and dimeric AmB-NaDC formulations were also characterised by Electron Microscopy, Fourier Transform Infrared Spectroscopy (FT-IR), Powder X-ray diffraction (PXRD), Differential Scanning Calorimetry (DSC), Modulated temperature DSC (MTDSC) and Thermogravimetric Analysis (TGA) [16]. A detailed description of the methodologies applied is provided in SI. 2. Characterization of AmB formulations.

In vitro stability in simulated gastrointestinal and intestinal fluids

Simulated gastric fluid (SGF, pH 1.2) and simulated intestinal fluid (SIF, pH 6.8) without enzymes were prepared as previously described [17]. AmB-NaDC and AmB-AME -(1 mg mL^{-1}, 250 µL) were suspended in prewarmed (37±0.5°C) SGF or SIF (100 mL) under gentle shaking (120 rpm) for a maximum of 3.5 h or 24 h respectively. At regular time intervals, aliquots (1 mL) were removed and AmB content and aggregation state was analysed by UV. The absorbance at 328 and 407 nm was used to quantify the AmB in both aggregation states, dimer and monomer. The calibration curve obtained in SGF was $y= 0.1116x-0.0249$ ($R^2= 0.9995$) and in SIF was $y=0.1016x+0.0315$ ($R^2= 0.9996$) (where y was absorbance and x was concentration in µg mL^{-1}). Experiments were performed in triplicate.

In vitro drug release

The release studies were carried out under sink conditions in 50 mL tubes containing phosphate buffer with 1% sodium deoxycholate (50 mM, 45 mL, pH 7.4 ±0.1), maintained at 37 ± 0.5 °C, with stirring at 50 rpm [18]. AmB or AmB-AME (equivalent to 5.0 mg of AmB) were dissolved in 5 ml of physiological sterile 0.9% saline and 5% glucose solutions (1:9 v/v) as used for *in vivo* studies and added to the release buffer (5 mL). At appropriate time intervals (5, 15, 30, 60, 120, 240, 300, 360 and 1440 min), samples (2 mL) were withdrawn and filtered through a 0.45 µm Millipore membrane filter

and analyzed using a validated HPLC assay [19]. The volume was replaced each time with fresh prewarmed medium to maintain sink conditions.

2.3. Trypanocidal assays

2.3.1. *In vitro* trypanocidal assay

Trypanosoma parasites are found in different forms during their life cycle. Trypomastigotes enter the host either through the wound originated from the triatomine insect vector or through intact mucosal membranes, such as the conjunctiva. Inside the host, the trypomastigotes invade cells near the site of inoculation, where they differentiate into intracellular amastigotes. The amastigotes multiply and differentiate into trypomastigotes, being released into the bloodstream infecting cells from a variety of tissues and transforming into intracellular amastigotes in new infection sites. The triatomines becomes infected by feeding on blood that contains trypomastigotes which transform into epimastigotes in the vector's midgut. The parasites multiply and differentiate into infective metacyclic trypomastigotes in the hindgut which will be transmitted in the next blood meal [20]. To test the *in vitro* efficacy of novel formulations, a standardized protocol for screening potential drugs for the treatment of Chagas disease was followed using epimastigotes and amastigotes because trypomastigotes are unable to replicate [21]. Screening using epimastigotes enables testing directly the efficacy of drugs / formulations against the parasite and amastigotes (intracellular forms) assesses the ability of the drug to permeate cellular membranes and remain effective against the amastigotes form of the parasite.

Parasites

The *T. cruzi* clone CL-B5 were kindly provided by Dr F Buckner through Instituto Conmemorativo Gorgas (Panama) and were stably transfected with the *Escherichia coli* β-galactosidase gene (lacZ). The epimastigotes were grown at 28 °C in liver infusion tryptose broth (complemented with 10% fetal bovine serum, FBS (Internegocios, Argentina), penicillin and streptomycin) and afterwards, were harvested during the exponential growth phase.

Epimastigote susceptibility assay

The assay was performed in 96-well microplates (Cellstar, E.E.U.U.) with cultures that have not reached the stationary phase, as was previously described [10a]. Briefly epimastigotes were seeded at a concentration of 2.5×10^5 per mL in a total volume of 200 µL. Plates were incubated with the formulations which were serially diluted 2-fold at 28 °C for 72 h. Then, chlorophenol red−β-D-galactopyranoside solution (50 µL - CPRG Roche, Indianapolis, IN) was added to obtain a final concentration of 200 µM. Plates were incubated for another 4 h at 37°C and then, were read at 595 nm. Benznidazole was used as a reference drug. Each concentration was tested in triplicate and each experiment was performed twice separately. The efficacy of each compound was estimated by calculating the IC_{50} (drug concentration that produces 50% reduction in parasites).

Amastigote susceptibility assay

The assay was performed by a colorimetric method using chlorophenol red−β-D-galactopyranoside (CPRG) [2, 10a]. Briefly, NCTC-929 fibroblasts [a gift from Dr Gomez-Barrio (Universidad Complutense de Madrid, Spain)] were cultured in 24-well tissue culture plates at a concentration of 2.5×10^3 cells/well which was previously optimised.

NCTC-929-derived trypomastigotes were added to the monolayers at a parasite: cell ratio of 5: 1 and were incubated for 24 h at 33 °C with 5% CO_2. In order to remove the extracellular trypomastigotes, the infected cells were then washed twice with PBS. The formulations were added in triplicate resulting in a final volume of 900 µL/well. Plates were incubated for 7 days at 33 °C. CPRG solution (100 µL) in 0.3% Triton X-100 was then added to obtain a final concentration of 400 µM. The colorimetric reaction was quantified by measuring optical density (OD) at 595 nm wavelength after 4 h of incubation at 37 °C.

The percentage of anti-amastigote activity (%AA) was expressed as indicated in Equation 1:

$$AA\ (\%) = 100 - \frac{\text{OD experimental wells}}{\text{OD control wells)}} \text{ x } 100 \qquad \text{(Eq. 1)}$$

Background controls (only NCTC- 929 cells) were subtracted from all values.

2.3.2. *In vivo* trypanocidal assay

All experiments were approved and performed in accordance with the local ethical committee of the Fundacion Moisés Bertoni (PROCIENCIA-14-INV-022, CONACYT-Paraguay). Bloodstream trypomastigotes of the Y strain (ATCC 50832) were used which were harvested from *T. cruzi* infected BALB/c mice on the day of peak parasitaemia as previously described [22]. Female 4-6 week old BALB/c mice (18−20 g) were obtained from the Animal Facility of the Instituto de Investigaciones en Ciencias de la Salud, Universidad Nacional de Asuncion (UNA, Paraguay). Mice were housed according to the standards of the Committee of Animal Welfare and were kept in a room at 20−24 °C under a 12/12 h light/dark cycle and provided with sterilized water and food *ad libitum*. The animals were allowed to acclimatise for 7 days before the onset of the experiments. Animals were infected by intraperitoneal injection of 10^4 Y strain trypomastigotes of *T. cruzi*.

Treatment

The experimental protocol performed allows the analysis of the effect of the AmB formulations on the parasite load [21]. Mice were randomly split into groups of ten to ensure that a 50% difference in parasitic load can be detected with 95% confidence. At day 5 post-infection, parasitaemia (number of trypomastigotes mL^{-1} of blood) was quantified microscopically using the Pizzi−Brener method [23]. Only animals that demonstrated homogeneous parasitaemia were used. In all the experiments, both a negative control group (untreated mice) and a reference group (treated with 100 mg/kg/day of benznidazole) were included. AmB formulations freshly diluted to 1 mg mL^{-1} using a mixture of physiological sterile 0.9% saline and 5% glucose solutions (1:9 v/v) were administered by intracardiac puncture at day 5 and 8 post-infection: poly-aggregated AmB at the dose of 2.5 and 5 mg kg^{-1}, AmB-AME at the dose of 2.5 and 5 mg kg^{-1} and dimeric AmB-NaDC at the dose of 0.5 mg kg^{-1}. Higher doses of dimeric AmB-NaDc were not used as it has been linked to animal mortality [5]. Intracardiac administration was used to spare the high potential risk of AmB thrombophlebitis (Goodwin, S.D. et al 1995 Clin Infect Dis 20(4):755-61.) and to avoid damage of the tail vein needed for sampling for analysis of the parasitaemia levels. Parasitaemia was quantified at 7, 9 and 12 days post-infection. In the second experiment, the effect of AmB AME dose and effect of single versus multiple administrations was studied. AmB-AME diluted as described above was administered by intracardiac injection as a single dose of 20 mg kg^{-1} at day 5 post-infection, or as two doses of 2.5 and 5 mg kg^{-1} at days 5 and 8 post-infection or as

three doses of 5 and 10 mg kg^{-1} at days 5, 8 and 11 post-infection. Parasitaemia was again quantified at 7, 9, and 12 days post-infection [21]. In a third experiment, fed animals were treated by oral gavage at day 5 post-infection with dimeric AmB-NaDC at a dose of 5, 10 or 15 mg kg^{-1} daily for 10 consecutive days. The formulation was freshly reconstituted with deionised water to 5 mg mL^{-1} and further diluted with 5% sterile glucose to 1 mg mL^{-1} prior to administration. Parasitaemia was quantified at 10, 14, and 17 days post-infection due to the longer duration of the oral treatment compared to parenteral regimens. Results from each tested formulation were compared to the control groups. The percentage of parasitaemia reduction was calculated using Equation 2:

$$\text{Parasitaemia reduction (\%)} = 100 - \left(\frac{PT}{PC}\right) x\ 100 \qquad \text{(Equation 2)}$$

where PC is the number of trypomastigotes mL^{-1} of blood in the control group and PT is the number of trypomastigotes mL^{-1} of blood in the treated group at the same day post-infection [10a]. The mice survival rate was recorded up until the end of the acute phase (30 days) in all the experiments.

2.4. Cytotoxicity assays

Fibroblast NCTC929 (as above) were used to assess the cytotoxicity of the formulations. The cells were grown in Minimum Essential Medium (MEM; Sigma, St. Lois, USA) supplemented with 10% FBS, 2 mM L-glutamine, and antibiotics (50 units mL^{-1} penicillin and 50 g mL^{-1} streptomycin) and cytotoxicity assays were performed as previously described [10a]. NCTC clone 929 cells were plated in 96-microtiter plates at 3×10^4 cells/well in 100 µL of growth medium and were grown overnight at 37 °C, 5% CO_2. Afterwards, the medium was removed and the serially diluted two-fold formulations were added in 200 µL of medium for 24 h, after which time resazurin solution (20 µL, 2 mM) was added to each well. The plates were incubated for a further 3 h and the absorbance was read at 570 and 595 nm on a microplate reader (Sinergy, Biotek, Vermont, USA). The cytotoxicity of the formulations was measured in terms of the concentration that was able to reduce the viability of treated cells in culture by 50% compared to untreated cells in culture (CC_{50}).

2.5. Statistics

SPSS 22 (IBM Corporation, New York, USA) software was used to perform Probit multilineal analysis to determine the parasite efficacy in terms of IC_{50} and cytotoxicity

313 (CC_{50}). Tukey's HSD post-hoc test and Mann-Whitney U test were used to analyse all
314 the *in vitro* and *in vivo* test data respectively. Statistical significance was considered at p
315 < 0.05 using Minitab 16 software (Minneapolis, USA). Statistical analysis of survival
316 data were performed using SPSS 22 (IBM Corporation, New York, US). The Log Rank
317 (Mantel-Cox) test was used to test whether differences in survival times between groups
318 are statistically different.

319 **3. Results**

320 **3.1. Preparation and characterization of AmB formulations**

321 AmB-NaDC spectra showed a broad intense band at 328-340 nm, characteristic of
322 dimeric AmB, while poly-aggregated AmB and AmB-AME displayed characteristic
323 bands of smaller intensity at 360–363, 383–385 and 406–420 nm (Figure 1a) [8]. This
324 difference lies on the fact that AmB contains conjugated pi-electrons in its structure. In
325 the AmB-NaDC, the AmB molecules are solubilised and the conjugated pi bond system
326 act as cromophores resulting in a strong UV absorbance. Poly-aggregated AmB has a
327 lower UV absorbance due to intermolecular interactions reducing electron movement
328 between energy levels.

329 AmB-NaDC illustrated a mixed morphology of spherical micelles and fibrils
330 (approximately 30 nm in length) (Figure 2b). After lyophilisation, thin sheets exhibiting
331 a smooth surface were observed (Figure 2c). A good yield was obtained for AmB-AME
332 ($73.4 \pm 4.3\%$) after spray-drying, with high AmB encapsulation efficiency ($82.1 \pm 6.5\%$)
333 and a hollow quasi-spherical particle morphology of between 1 and 10 μm in diameter
334 (Figure 2g). Networks of long axial fibrils were observed for AmB-AME after
335 reconstitution in de-ionised water. In contrast, poly-aggregated AmB appeared as needle-
336 like crystals (100 - 3,500 nm, Figure 2d), a morphology that remained unaltered post
337 lyophilisation (Figure 2e). See Table S1 in Supplementary material for further details.

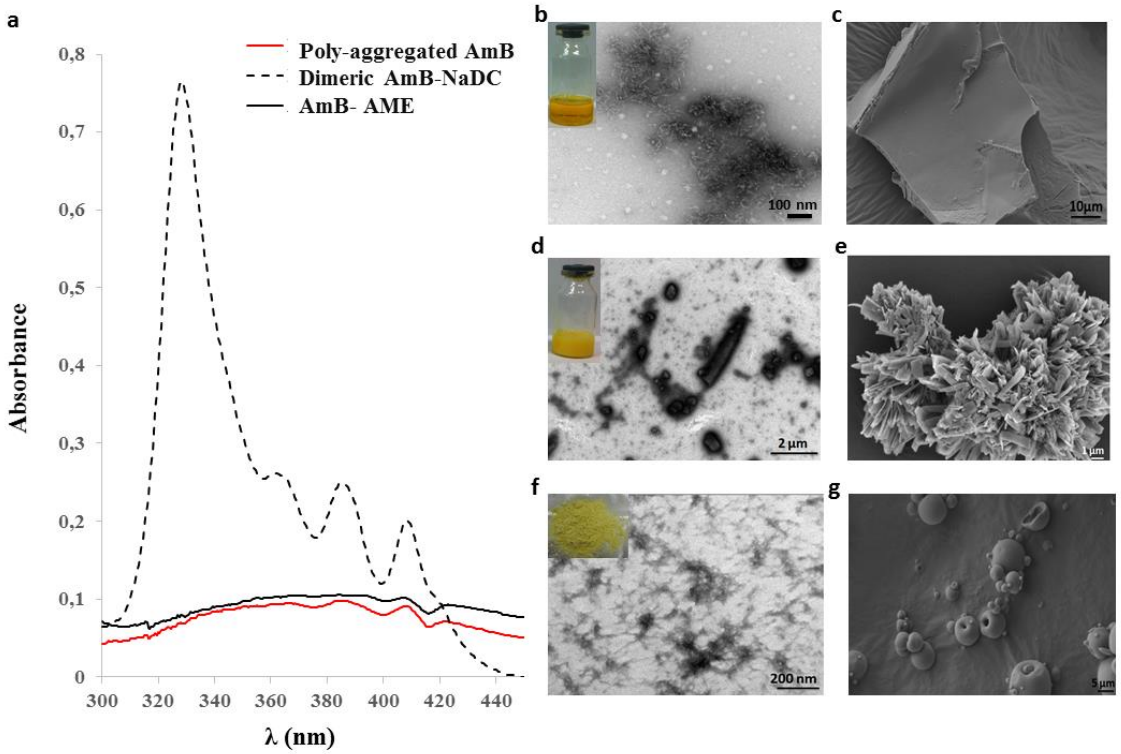

Figure 1. **AmB aggregation state and morphology of AmB formulations.** Key: a) AmB aggregation state of poly-aggregated AmB, dimeric AmB-NaDC and AmB-AME; b) TEM of dimeric AmB-NaDC, Bar: 100 nm; c) SEM of freeze-dried dimeric AmB-NaDC, Bar: 10 µm; d) TEM of poly-aggregated AmB, Bar: 2 µm; e) SEM of freeze dried poly-aggregated AmB, Bar: 1 µm; f) TEM of AmB-AME, Bar: 200 nm; g) SEM of spray-dried AmB-AME, Bar: 5 µm. Samples were negatively stained with 1% w/v aqueous uranyl acetate solution for TEM images. Inserts in images a, c, and e illustrate the appearance of the formulation.

FT-IR spectra indicate amorphization of AmB in both AmB-NaDC and AmB-AME formulations (Figure 2). The spectrum obtained for AmB was similar to previously published reports [24], while AmB-NaDC was characterized by broader bands attributed to AmB amorphization as a result of lyophilisation. The absence of a peak at 1691 cm^{-1} assigned to the carboxylate group of AmB (C=O stretching) in the AmB-NaDC (Figure 2A iii) compared to the physical mixture (Figure 2A iv) indicates an ~~electrostatic~~ interaction between AmB and NaDC [6b]. AmB-AME also illustrated broader bands probably due to amorphization as a result of spray drying [25]. The disappearance of the carboxylate group peak at 1691 cm^{-1} ν (C=O stretching) and the amine peak of the AmB at 1552 cm^{-1} δ (N-H bending) can be attributed to electrostatic interactions with the AME.

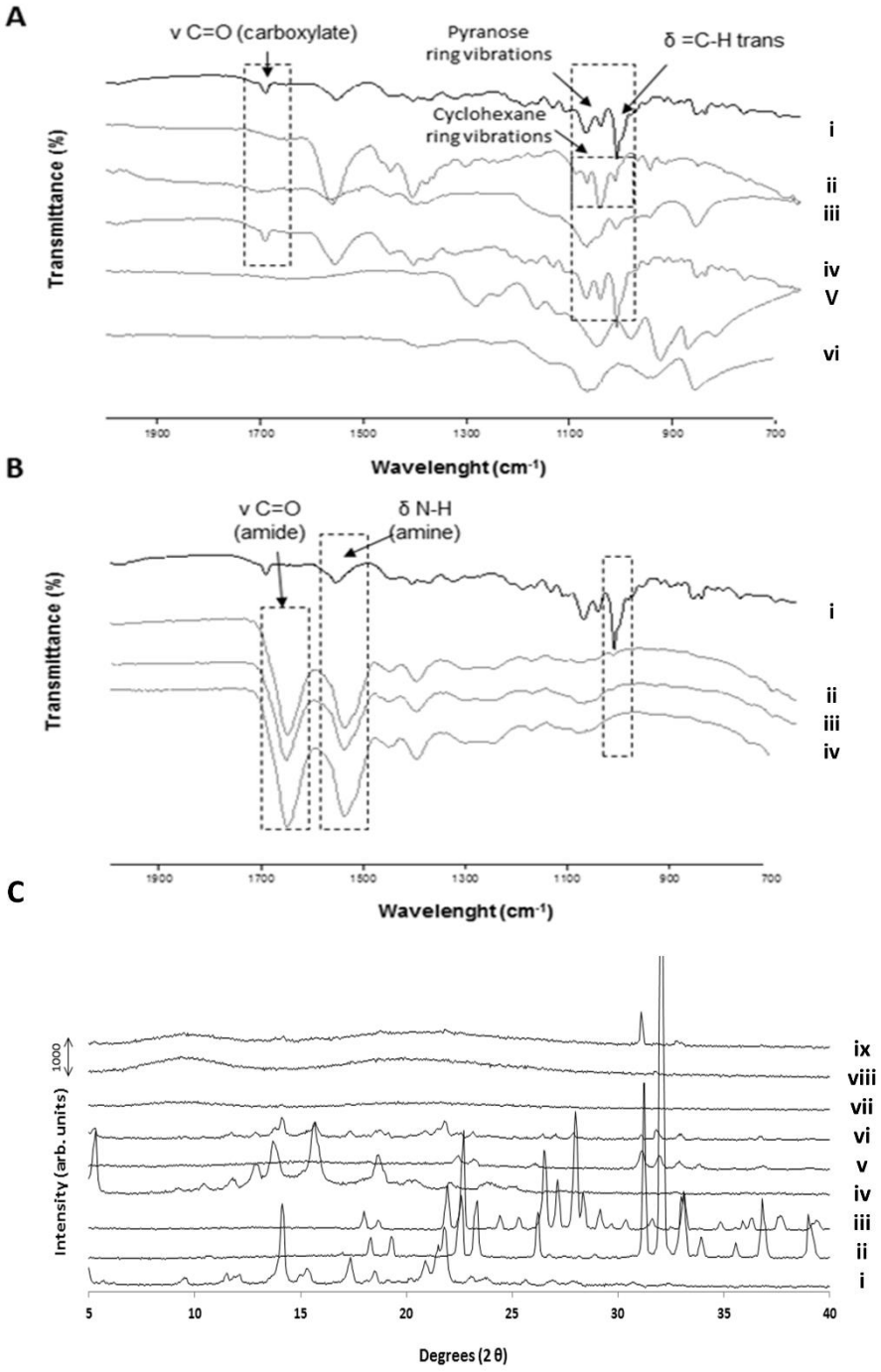

359

360 **Figure 2**. **FTIR spectra and PXRD pattern of AmB formulations**. A) FTIR spectra of
361 dimeric AmB-NaDC formulation and starting materials: i) AmB starting material; ii)
362 NaDC starting material; iii) lyophilised dimeric AmB-NaDC; iv) physical mixture
363 containing all starting materials of the dimeric AmB formulation; v) Monobasic sodium
364 phosphate starting material; vi) Dibasic sodium phosphate starting material. Key: δ,
365 bending vibrations; ν, stretching vibrations. B) FTIR spectra of AmB-AME formulation
366 and starting materials: i) AmB; ii) Physical mixture of AmB and blank spray dried
367 albumin microspheres; iii) spray dried AmB-AME and iv) blank spray dried albumin
368 microspheres (AME). Key: δ, bending vibrations; ν, stretching vibrations. C) PXRD
369 patterns of dimeric AmB-NaDC and poly-aggregated AMB-AME formulations. Key: i)

AmB starting material; ii) Na_2HPO_4 starting material; iii) NaH_2PO_4 starting material; iv) NaDC starting material; v) AmB-NaDC lyophilized; vi) Physical mixture of AmB and NaDC starting materials; vii) Spray dried AmB-AME; viii) AME; ix) Physical mixture of AmB and AME starting materials.

The signal corresponding to polyenic double bonds (=C-H trans bending at 1007 cm^{-1}) of AmB was present in the spectrum of the physical mixture but not in that of the AmB-AME, which is indicative of drug entrapment within the microparticles.

PXRD analysis confirmed the crystalline nature of the AmB (Figure 2C) and the rest of the excipients (NaDC, Na_2HPO_4, NaH_2PO_4), except for the blank spray dried albumin microspheres (AME) (Figures 2C ii-iv, viii). AmB-AME showed a characteristic amorphous halo (Figure 2C vii) whereas the physical mixture of AmB and AME starting materials revealed the presence of crystalline drug even at low concentration (4 % w/w) and also crystalline NaDC and phosphate salts (Figure 2C viii). Several Bragg peaks were observed in the dimeric AmB-NaDC formulation (Figure 2C v); however, they are related to phosphate salts and no indication of characteristic peaks of crystalline AmB (2θ, 14.15, 17.35 and 21.8) were detected in the lyophilised formulation, unlike the physical mixture of AmB and NaDC, where AmB and other excipient peaks were clearly observed (Figure 2C vi).

The water sorption kinetic profiles of the lyophilised AmB-NaDC formulation, the spray dried AmB-AME and AmB (crystalline) are shown in Figures 3a-c. AmB showed an increase in mass of approximately 8% at 90% relative humidity (RH), whereas lyophilised AmB-NaDC and AmB-AME showed a mass increase of 60% and 40% respectively at the same RH. AmB-NaDC exhibited a mass loss at 70% RH in the first sorption cycle and above 30% RH in the second sorption cycle. However, AmB within the AmB-NaDC sample remained amorphous after DVS analysis and the mass loss is attributed to crystallization of the phosphate salts, which was verified by PXRD (Figure 3d). AmB-AME showed no mass loss in any sorption cycle and the PXRD pattern exhibited an amorphous halo after the DVS analysis.

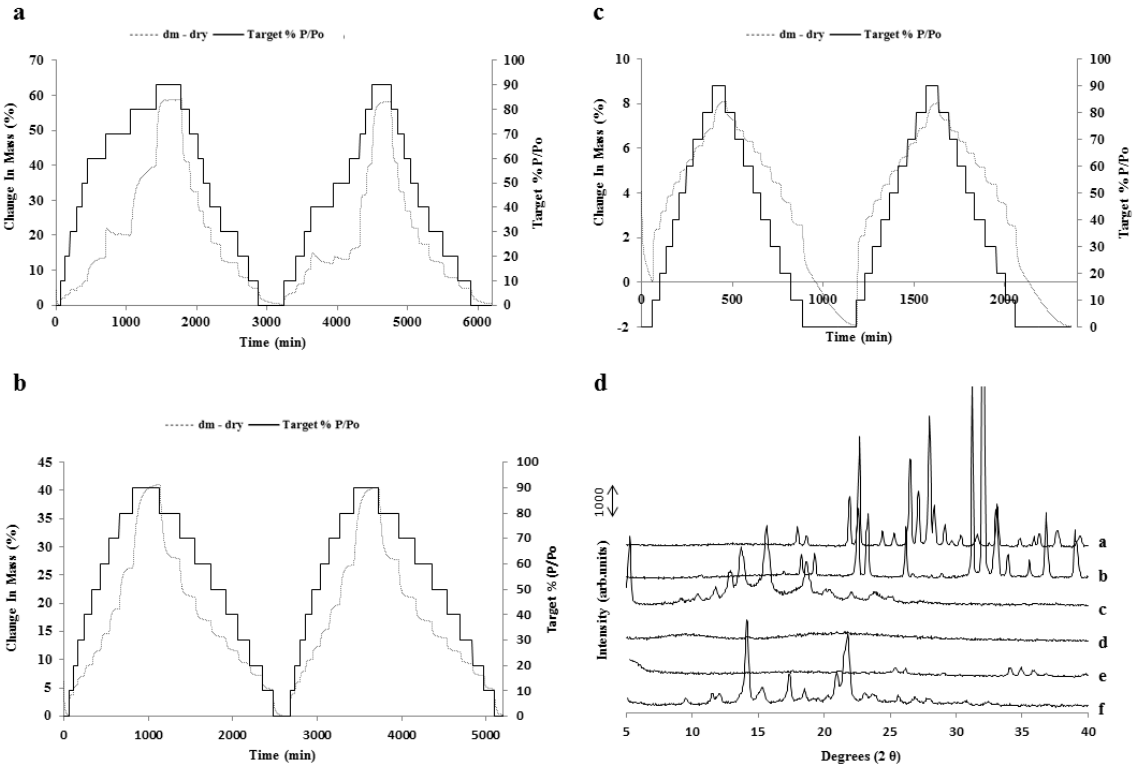

398

399 **Figure 3**. **Water sorption kinetics profiles** for: a) Dimeric lyophilized AmB-NaDC, b)
400 Spray dried AmB-AME; c) AmB (crystalline); **d) PXRD patterns after DVS**
401 **experiments:** Key: a) NaH_2PO_4; b) Na_2HPO_4; c) NaDC; d) Spray dried AmB-AME; e)
402 AmB-NaDC lyophilised and f) AmB.

403 Thermal analysis illustrated that AmB exhibited a characteristic endothermic peak at 96.5
404 ºC which is attributed to water loss [26], as verified by thermogravimetric analysis (6.2%
405 loss of water) (Figure 4), and started to decompose above 160 ºC which obscured the
406 endothermic peak corresponding to the melting of the drug at approximately 169 ºC [26a].
407 MTDSC analysis confirmed a second endothermic event for the drug at 170 ºC in the
408 reversing heat flow signal (Figure S1, see SI.4. Results). The AmB-AME formulation
409 showed a dehydration peak corresponding to 2.4% water loss followed by a broad melting
410 peak at 200.3 ºC ($\Delta H_f = 41.1 \pm 1.2$ J g^{-1}). Decomposition of AmB-AME occurred at higher
411 temperatures compared to the drug alone (> 220 ºC). Both the AME and the physical
412 mixture of AmB with AME showed a similar DSC profile as the AmB-AME formulation;
413 however, the TGA curve of the physical mixture components showed a higher weight
414 loss (9.6 %) in the temperature range of 25 – 100 ºC. Anhydrous NaH_2PO_4 was
415 transformed to pyrophosphate at 210 ºC [27], which corresponds to the weight loss at this
416 temperature in the TGA curve. NaDC (dihydrate) was converted to the amorphous
417 anhydrous form (dehydrated NaDC) by drying above 60 ºC corresponding with 10.4%

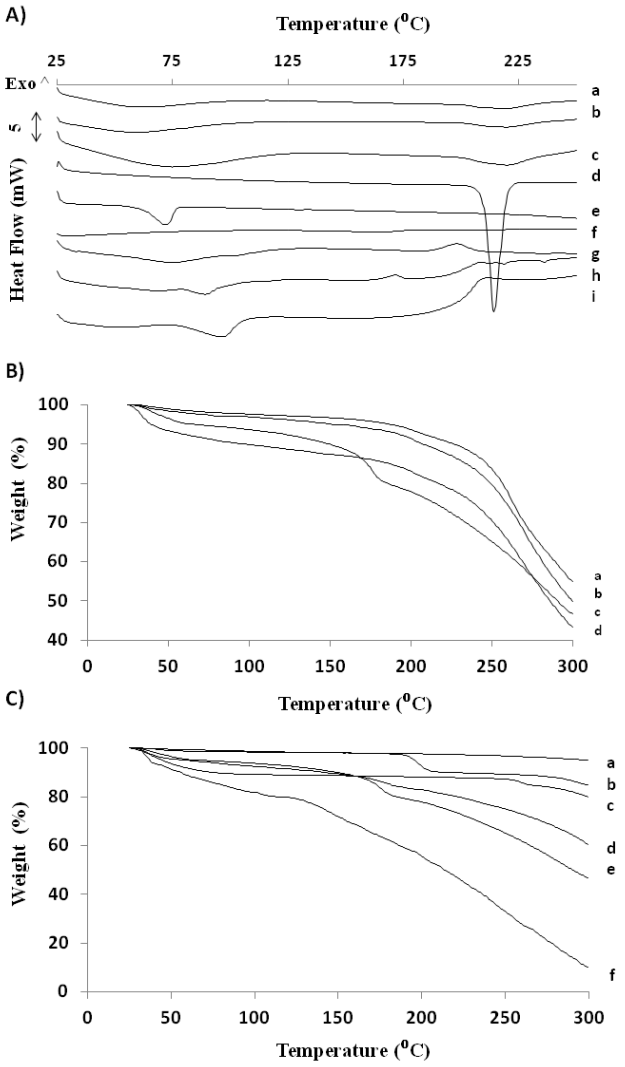

418

419 **Figure 4. Thermal analysis of dimeric AmB-NaDC and poly-aggregated AmB-AME**
420 **formulations.** A) DSC thermograms; Key: a- AME; b- Physical mixture of AmB and
421 AME; c- Spray dried AmB-AME; d– sodium dihydrogen phosphate (NaH_2PO_4); e–
422 Disodium hydrogen phosphate (Na_2HPO_4); f– lyophilized AmB-NaDC; g- NaDC; h-
423 Physical mixture of AmB and NaDC; i- AmB. B) TGA curves; Key: a- Spray dried AmB-
424 AME; b- Blank AME; c– AmB; d- Physical mixture of AmB and AME; C) TGA curves.
425 Key: a– Disodium hydrogen phosphate (Na_2HPO_4); b– sodium dihydrogen phosphate
426 (NaH_2PO_4); c- NaDC; d- Physical mixture of AmB and NaDC; e- AmB; f– lyophilized
427 AmB-NaDC.

428 weight loss in the temperature range of 25-100 °C. The amorphous anhydrous form of
429 NaDC exhibited an exothermic event at 197.9 °C (ΔH_c= 35.7 ± 2.3 J g^{-1}) crystallizing to
430 anhydrous crystalline NaDC. Similar results were reported by other authors [28]. The
431 physical mixture of AmB and NaDC exhibited a double endothermic peak below 100 °C
432 related to water loss from both AmB and NaDC. The exothermic event related to the
433 crystallization of the amorphous anhydrous NaDC was shifted to a lower temperature

(164.2 ºC). No thermal events were observed in the lyophilised AmB-NaDC formulation; however, an earlier decomposition was observed at above 125 ºC.

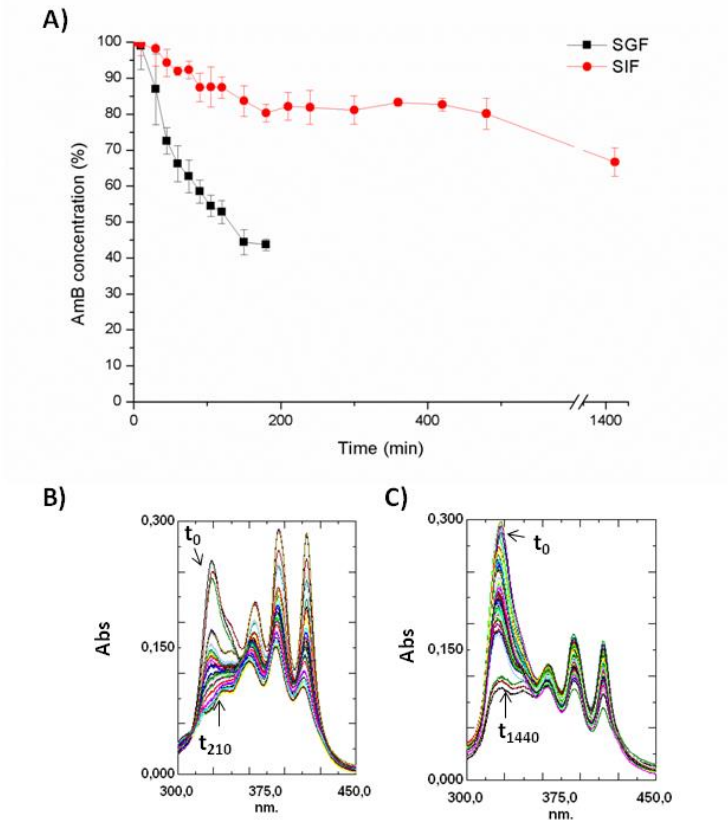

Figure 5. ***In vitro*** **stability in simulated gastrointestinal and intestinal fluids of AmB-NaDC**. A) AmB content; B) AmB aggregation state in SGF; C) AmB aggregation state in SIF. The initial aggregation state (t_0) and the aggregation state at the end of the experiment (210 min in SGF and 1440 min in SIF) are indicated in figures B and C.

AmB-NaDC and AmB-AME were more stable in SIF than SGF, with 10-15% of the drug degrading/precipitating in 30 min in SGF, while more than 80% remained after 8 hours of incubation in SIF (Fig. 5A and Figure S2A). These results are in agreement with other authors who suggested that the stability of the drug in aqueous media at pH below 4 or higher than 10 was poor [29]. AmB-NaDC illustrated similar absorbance at 328 and 407 nm (ratio $_{328/407} \approx 1$) in SGF indicating the presence of both AmB dimeric and monomeric aggregation states in equilibrium at early time points (Figure 5B). After 10 min in SGF, the absorbance at 328 nm decreased and the ratio $_{328/407}$ was shifted to values of 0.6 indicating degradation and a conversion of dimeric aggregates at acid pH towards the monomeric state, as AmB has higher solubility at acidic pH. The transformation from dimer to monomer also explains the faster degradation of the drug in SGF compare to

SIF. In SIF, up until 8 hours, AmB is present predominantly as a dimer ($Abs_{328} > Abs_{407}$), which is the more stable form, as indicated by the >80% AmB remaining at this time point. At time 0, the ratio $_{328/407}$ was 2.8 which was slowly decreasing. After 8 h, the ratio $_{328/407} \approx 1$. Although AmB-AME were designed for parenteral administration, we also decided to compare their stability in SGF and SIF. AmB-AME showed an immediate transformation to a monomeric form in acid media probably indicating a dissociation from the albumin that led to a faster degradation (Figure 2SB). In SIF, AmB remained as a poly-aggregate due to its low solubility at this pH, which would likely hamper its oral absorption. For this reason, only the efficacy of AmB-NaDC after oral administration was tested *in vivo*.

AmB aqueous suspension showed a limited release in PBS (pH 7.4) due to the low aqueous solubility at physiological pH (<50 μg mL^{-1}). AmB-AME showed an initial burst release in PBS at pH 7.4 (25% within 15 minutes), after which the levels remain stable throughout the duration of the experiment indicating an equilibrium between the drug bound to albumin and the free drug in solution (poly-aggregate) (Figure 6, Figure S3). At 24 h a decrease in the AmB levels was observed which could be probably explained by the degradation of the drug in aqueous media at 37ºC.

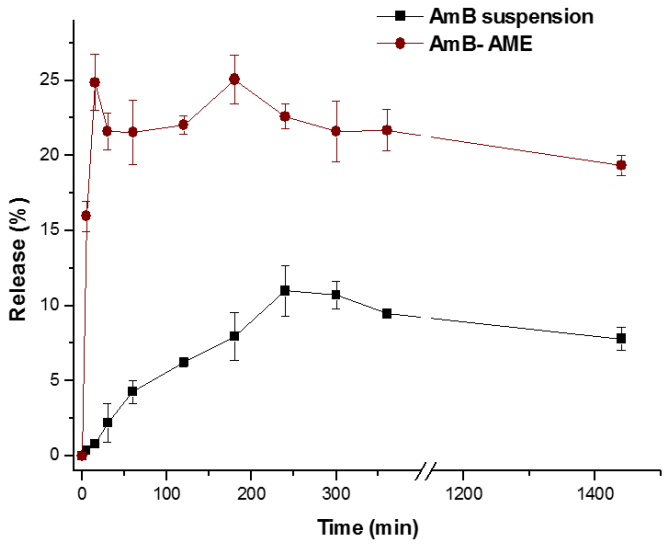

Figure 6. *In vitro* drug relelease (%) profile for AmB-AME compared to AmB suspension. Key: AmB-AME diluted to 1 mg mL^{-1} in a mixture of physiological sterile 0.9% saline and 5% glucose solutions (1:9 v/v) (brown circle); AmB suspension prepared after dilution of the drug to 1 mg mL^{-1} in the same mixture (black square).

3.2. In vitro activity against *T. cruzi* and cytotoxicity assay

All formulations displayed promising IC_{50} values against *T. cruzi* against both epimastigotes and amastigotes (Table 1). Good selectivity index against epimastigotes (CC_{50}/IC_{50}) were obtained resulting in 280, 175 and 236 higher selectivity for AmB-NaDC, poly-aggregated AmB and AmB-AME respectively. Also, AmB formulations exhibited much greater activity against epimastigotes than the existing approved drugs to treat trypanosomiasis (18-30-fold higher than benznidazole and between 7-12 fold higher than nifurtimox, depending on the parasite strain). Lower cytotoxicity against fibroblasts was observed when poly-aggregated AmB was encapsulated in AME resulting in a promising therapeutic formulation with a 1.4 and 1.7-fold higher selectivity index. However, the greatest activity and selectivity index against amastigotes was observed for AmB-NaDC (8.6 and 11.5-fold higher than nifurtimox and benznidazole respectively) while moderate selectivity index was shown for poly-aggregated AmB and AmB-AME respectively, possibly due to the inability of larger poly-aggregated AmB and AmB-AME particles to permeate across cellular membranes.

Table 1. Trypanocidal activity of AmB formulations on extracellular and intracellular *T.cruzi* forms and cytotoxicity on NCTC929 fibroblasts.

Formulation	Epimastigotes IC_{50} (μg mL^{-1})	SI against epimastigotes	Amastigotes IC_{50} (μg mL^{-1})	SI against amastigotes	NCTC929 Fibroblasts CC_{50} (μg mL^{-1})
AmB-NaDC	0.79	280.3	0.07	3164	221.5
Poly-aggregated AmB	0.55	175.4	10.6	9.1	96.5
AmB-AME	0.47	236.4	7.04	15.8	111.1
Benznidazole	14.2	11.7	0.6	275.8	165.5
Nifurtimox	5.5	16	<0.25	>353	88.3

Key: IC_{50}, AmB concentration that produced a 50% reduction in parasites; CC_{50}, AmB concentration that produced a 50% reduction of cell viability in treated culture cells with respect to untreated ones; SI, selectivity index calculated as the ratio between the CC_{50} and the IC_{50}.

3.3. In vivo activity

The parasitaemia levels after parenteral administration of AmB formulations [AmB-NaDC (0.5 mg kg^{-1}), AmB-AME (2.5 and 5 mg kg^{-1}) or poly-aggregated AmB (2.5 and 5 mg kg^{-1})] at days 5 and 8 post-infection were quantified during the acute infection period

at days 7, 9 and 12 post-infection (Figure 7, Figure S4). Dimeric AmB-NaDC did not significantly reduce the number of trypomastigotes per mL at any time compared to the control group due to the low AmB tolerated dose, but was, however, able to increase the median survival time compared to the control group (Figure 7b from 23 days for control group to 26 days for AmB-NaDC). Higher doses of AmB-NaDC were not tested as they have been shown to lead to high animal mortality mainly due to arrhythmia and bronchospasm [5, 7]. Poly-aggregated AmB and poly-aggregated AmB encapsulated in AME allowed administration of higher doses and significantly reduced the parasitaemia levels by 2 and 3.6 fold respectively compared to the control group at day 7 post-infection. Nevertheless, an increase in parasitaemia was observed after the second dose of both formulations which could be related to a lack of activity of this low AmB dose compared to previously published reports which utilised either 5-fold higher intravenous [11a] or intraperitoneal doses (leading to slower clearance) and longer treatment regimens [11b]. Poly-aggregated AmB formulations have a higher tissue distribution (180-fold higher than AmBisome®) [8], which to an extent explains their low activity against the level of parasites present in the blood [8]. Survival was prolonged compared to the control group only when AmB, either in the poly-aggregated form (AmB-NaDC) or encapsulated in albumin (AmB-AME), was administered at doses of 5 mg $k6g^{-1}$ (Median survival time for the control group 23 days was raised to 25 days with AmB-AME and 26 with poly-aggregated AmB).

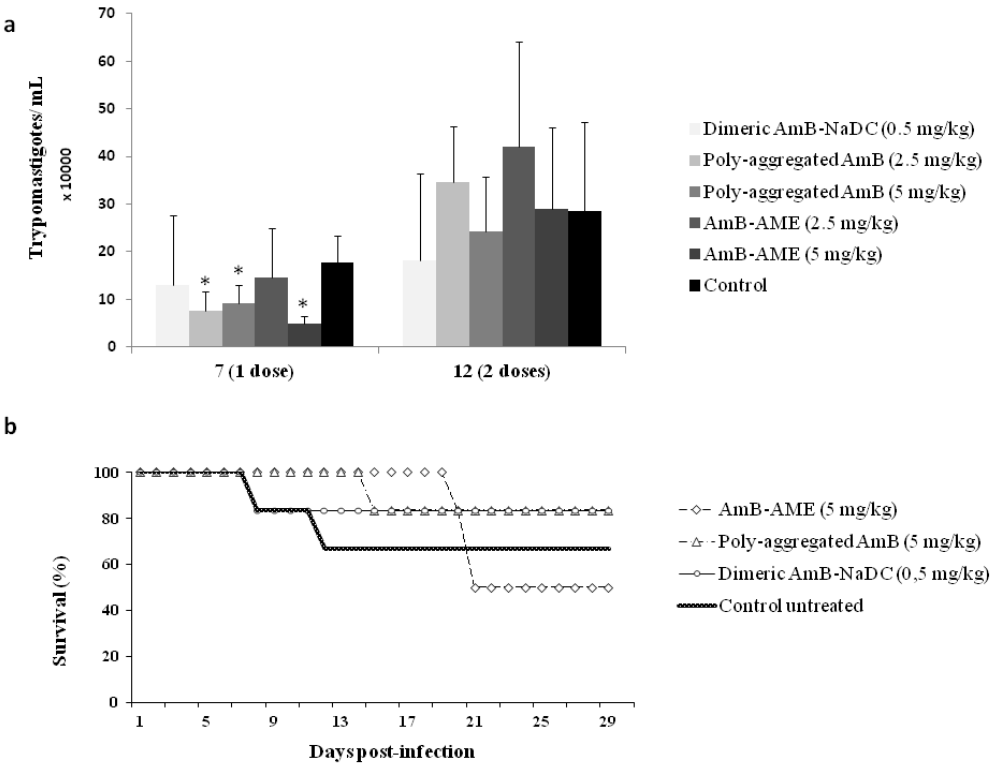

Figure 7. a) Parasitaemia levels during the acute infection period (days 7 and 12 post-infection) in BALB/c male mice infected with 10,000 bloodstream trypomastigotes of *T. cruzi*. Mice were randomly split into groups of twelve to ensure that a 50% difference in parasitic load can be detected with 95% confidence. Mice received two doses of AmB at days 5 and 8 post-infection. Parasitaemia was determined by counting the number of trypomastigotes in 5 µL of fresh blood collected from the tail (means ± SEMs). Reference group treated with benznidazole (100 mg/kg/day) reduced 100% the parasitaemia at day 8 post-infection. Key: *$p < 0.05$ versus control. Bar labels (left to right): dimeric AmB-NaDC (0.5 mg kg^{-1}), poly-aggregated AmB (2.5 mg kg^{-1}), poly-aggregated AmB (5 mg kg^{-1}), AmB-AME (2.5 mg kg^{-1}), AmB-AME (5 mg kg^{-1}) and control. **b) Kaplan-Meier survival plot comparing the control versus parenteral administration of AmB formulations**. AmB-AME and poly-aggregated AmB at 2.5 mg kg^{-1} did not improve survival more than the control group and have not been represented in the graph. No statistical differences in between parenteral formulations were observed (Log-Rank test, $p>0.05$).

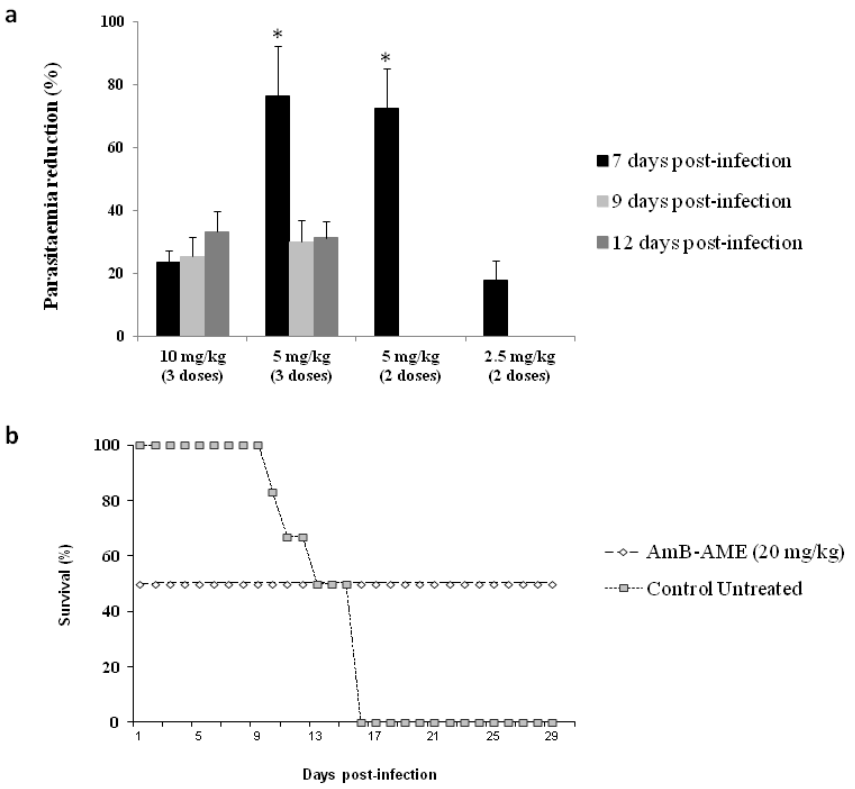

538

539 **Figure 8. a) *In vivo* efficacy after parenteral administration of AmB-AME at**
540 **different doses expressed as percentage of parasitaemia reduction.** Mice were
541 randomly split into groups of twelve to ensure that a 50% difference in parasitic load can
542 be detected with 95% confidence. Key: *p< 0.05 at 7 days post-infection. **B) Kaplan-**
543 **Meier survival plot comparing the control versus parenteral administration of**
544 **AmB-AME at 20 mg kg^{-1}.** No statistical differences in between parenteral formulations
545 were observed (Log-Rank test, p>0.05).

546 Administration of higher doses (3 doses of 5 and 10 mg kg^{-1}) of AmB-AME compared to
547 two doses of 2.5 and 5 mg kg^{-1}, that reduced the parasitaemia levels only at 7 days post-
548 infection, was more effective and decreased the trypanomastigotes mL^{-1} not only at day
549 7 post-infection, but also at days 9 and 12 (Figure 8a, Figure S5). However, the
550 administration of a single dose of AmB-AME at 20 mg kg^{-1} was not tolerated, as-observed
551 in the Kaplan-Meier survival plot (Figure 8b). However, it increased median survival time
552 from 13 days (control) to 15 days. Fifty percent of the animals died after the first day
553 post-treatment. Nevertheless, those animals that survived (n=5) after the first
554 administration survived longer (2-fold increase in survival) compared to the control
555 group. As formulations were administered intracardiacally, further experiments are
556 needed with these formulations to assess the LD_{50} after intravenous administration, which

can potentially minimize infusion-related side effects as a consequence of pro-inflammatory cytokine production [30].

Oral administration of the micellar AmB dispersion (AmB-NaDC) enabled a higher dose to be administered. Doses of 5, 10 and 15 mg kg^{-1} were administered with no clinical evidence of toxicity such as gross weight loss in any of the animals at the end of the experiment (Figure 9, Figure S6). Oral administration of AmB-NaDC at 5 mg kg^{-1} for 10 consecutive days resulted in a moderate reduction in parasitaemia levels (in the range of 20-30 %) whereas higher doses led to a greater parasitaemia reduction (> 75%) at day 17 post-infection. The administration of 10 mg kg^{-1} resulted in a higher reduction in parasitaemia earlier and was well tolerated ($p< 0.05$). At all doses, the survival rates were 100% (Figure 9b).

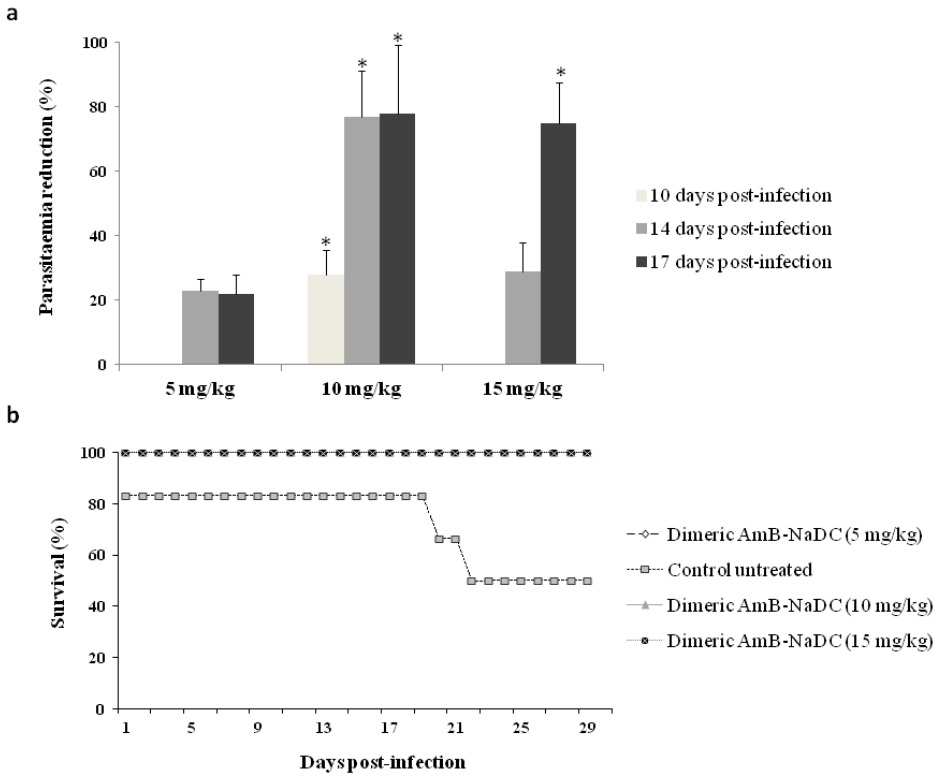

Figure 9. **a) Efficacy of oral dimeric AmB-NaDC formulation administered at the following doses of 5, 10 and 15 mg/kg for 10 consecutive days.** Mice were randomly split into groups of twelve to ensure that a 50% difference in parasitic load can be detected with 95% confidence. Key: *$p< 0.05$**. B) Kaplan-Meier survival plot comparing the control untreated versus different doses of dimeric AmB-NaDC.** All treatments consisting on dimeric AmB-NaDC led to 100% survival at the end of the acute infection period. AmB-NaDC is superior in prolonging survival versus control even at low oral doses (5mg/kg) (Log-Rank test, $p<0.0001$).

4. Discussion

AmB is a broad-spectrum antifungal and antiprotozoal drug with a low incidence of clinical resistance, however its use is limited by its high toxicity, especially nephrotoxicity, infusion-related side effects such as thrombophlebitis, fever, vomiting, headache and haemolysis, and its poor aqueous solubility, permeability and oral bioavailability. In order to overcome these issues, amorphous amphotericin B delivery systems were prepared by two different processes: i) spray-drying allowing the encapsulation of poly-aggregated AmB into albumin microspheres and ii) entrapment at the molecular level within NaDC micelles followed by lyophilisation. The amorphous nature of both formulations (AmB-NaDC and AmB-AME) was confirmed by the absence of the characteristic Bragg peaks of the drug in the PXRD patterns, the absence of endothermic events corresponding to the melting of crystalline drug in the DSC thermograms and no loss of mass associated with drug crystallization even at high relative humidities in DVS analysis.

No oral AmB dosage form is currently marketed, although many research efforts are focused on developing novel oral formulations to treat fungal diseases such as candidiasis and aspergillosis or leishmaniasis [6b, 31]. However, this is the first time that the oral efficacy of AmB against trypanosomiasis has been reported. This formulation may prove to be very beneficial, as the gastrointestinal lesions, such as mega-oesophagus and mega-colon, that have been described as the primary manifestations during the digestive form of the disease, can be directly targeted with an oral treatment [32]. Additionally, NaDC micelles facilitate the drug solubilisation and stability in the intestinal tract which is necessary to ensure AmB is available for absorption and to elicit its effect on the parasite membrane through pore formation after interaction with ergosterol [6a]. AmB-NaDC showed a high SI (>3000) *in vitro* compared to benznidazole and nifurtimox, both of which demonstrated activities in agreement with values previously reported [2, 33]. Although parenterally only low doses of 0.5 mg kg^{-1} of AmB-NaDC were tolerated, with limited ability to control parasitaemia in the acute phase, higher doses of up to 15 mg kg^{-1} were administered orally with no clinical evidence of toxicity (Figure 9, Figure S6). In previous pharmacokinetic studies [6b], the oral administration of AmB-NaDC (5 mg kg^{-1}) led to C_{max} of 0.25 µg mL^{-1} in plasma and 0.9, 0.8 and 0.75 µg g^{-1} in liver, spleen and lung respectively, which are well above the *in vitro* IC_{50} against amastigotes. To achieve the highest reduction in parasitaemia

level, a dose of 10 mg kg^{-1} of AmB-NaDC is required, making this formulation a promising cost-effective oral strategy to treat trypanosomiasis.

As a safer alternative to AmB-NaDC for parenteral administration, poly-aggregated AmB formulations, containing the least toxic aggregation state of the drug [5], have been proposed, either as free poly-aggregates or bound to albumin microspheres, resulting in formulations with higher volume of distribution for AmB and reducing its renal excretion and nephrotoxicity [8, 15, 34]. For this reason, parenterally administered poly-aggregated AmB formulations were better tolerated compared to AmB-NaDC micelles (0.5 mg kg^{-1}). Both poly-aggregates and AmB-AME displayed similar IC_{50} values in the nanomolar range with higher SI against epimastigotes than benznidazole and nifurtimox (used only for screening purposes) and a moderate SI against amastigotes. However, toxicity associated with parenteral administration was also observed with AmB-AME, which can be attributed to CD cardiomyopathy [14] making them more susceptible to AmB infusion-related side effects [30]. Survival was prolonged compared to control groups only when poly-aggregated AmB was administered at doses of 5 mg kg^{-1}.

5. Conclusions

CD affects more than 10 million people necessitating the emergence of safer, cost-effective and short duration oral treatments. Based on the *in vitro* and *in vivo* studies presented in the current work, the oral administration of an amorphous AmB-NaDC micellar dispersion (10-15 mg kg^{-1} day^{-1} for 10 days) represents a cost-effective, well tolerated therapy for trypanosomiasis, resulting in a 75% reduction of the parasitaemia levels and prolonging survival in the acute phase of the disease. Further studies are planned to assess the effects in the chronic phase of the disease. The use of the least toxic aggregation state of AmB in the treatment of CD was studied after parenteral administration, and poly-aggregated AmB-AME formulations (at a dose of 5mg kg^{-1}) were able to increase survival and reduce the parasitaemia levels by 3.6 fold at day 7 post-infection in the acute phase, compared to the dimeric form of AmB (AmB-NaDC). Pharmacokinetic studies of the AmB-NaDC are under way in order to support the clinical development of a cost-effective and orally bioavailable AmB treatment for CD worldwide.

Acknowledgements

This work was financial supported by Spanish Ministry of Ministry of Foreign Affairs and Cooperation (Project MAEC-AP/038991/11), and National Council of Science and Technology of Paraguay (PROCIENCIA-14-INV-022, CONACYT). D.R. Serrano is supported by a Research Fellowship FPU grant (AP2008-00235) from the Spanish Ministry of Education. C.V. and M.R. are grateful to PRONII/CONACYT (National Researchers Incentive Program / National Council of Science and Technology, Paraguay). AM Healy is supported by Science Foundation Ireland (SFI) under Grant Number SFI/12/RC/2275.

References

1. WHO, Chagas disease (American trypanosomiasis). Available from: http://www.who.int/mediacentre/factsheets/fs340/en/. Accessed date: 17/02/2016. **2015**.
2. Galiana-Rosello, C.; Bilbao-Ramos, P.; Dea-Ayuela, M. A.; Rolon, M.; Vega, C.; Bolas-Fernandez, F.; Garcia-Espana, E.; Alfonso, J.; Coronel, C.; Gonzalez-Rosende, M. E., In vitro and in vivo antileishmanial and trypanocidal studies of new N-benzene- and N-naphthalenesulfonamide derivatives. *Journal of medicinal chemistry* **2013,** *56* (22), 8984-98.
3. Croft, S. L.; Barrett, M. P.; Urbina, J. A., Chemotherapy of trypanosomiases and leishmaniasis. *Trends in parasitology* **2005,** *21* (11), 508-12.
4. Castro, J. A.; Diaz de Toranzo, E. G., Toxic effects of nifurtimox and benznidazole, two drugs used against American trypanosomiasis (Chagas' disease). *Biomedical and environmental sciences : BES* **1988,** *1* (1), 19-33.
5. Espada, R.; Valdespina, S.; Alfonso, C.; Rivas, G.; Ballesteros, M. P.; Torrado, J. J., Effect of aggregation state on the toxicity of different amphotericin B preparations. *International journal of pharmaceutics* **2008,** *361* (1-2), 64-9.
6. (a) Torrado, J. J.; Espada, R.; Ballesteros, M. P.; Torrado-Santiago, S., Amphotericin B formulations and drug targeting. *Journal of pharmaceutical sciences* **2008,** *97* (7), 2405-25; (b) Serrano, D. R.; Lalatsa, A.; Dea-Ayuela, M. A.; Bilbao-Ramos, P. E.; Garrett, N. L.; Moger, J.; Guarro, J.; Capilla, J.; Ballesteros, M. P.; Schatzlein, A. G.; Bolas, F.; Torrado, J. J.; Uchegbu, I. F., Oral particle uptake and organ targeting drives the activity of amphotericin B nanoparticles. *Molecular pharmaceutics* **2015,** *12* (2), 420-31.
7. Espada, R.; Valdespina, S.; Molero, G.; Dea, M. A.; Ballesteros, M. P.; Torrado, J. J., Efficacy of alternative dosing regimens of poly-aggregated amphotericin B. *International journal of antimicrobial agents* **2008,** *32* (1), 55-61.
8. Serrano, D. R.; Hernandez, L.; Fleire, L.; Gonzalez-Alvarez, I.; Montoya, A.; Ballesteros, M. P.; Dea-Ayuela, M. A.; Miro, G.; Bolas-Fernandez, F.; Torrado, J. J., Hemolytic and pharmacokinetic studies of liposomal and particulate amphotericin B formulations. *International journal of pharmaceutics* **2013,** *447* (1-2), 38-46.
9. Abitbol, H.; Pattini, R. E.; Salvador, J., [The "in vitro" action of amphotericin B on Trypanosoma cruzi]. *Revista de la Sociedad Argentina de Biologia* **1960,** *36*, 41-4.
10. (a) Rolon, M.; Seco, E. M.; Vega, C.; Nogal, J. J.; Escario, J. A.; Gomez-Barrio, A.; Malpartida, F., Selective activity of polyene macrolides produced by genetically modified Streptomyces on Trypanosoma cruzi. *International journal of antimicrobial agents* **2006,** *28* (2),

683 104-9; (b) Croft, S. L.; Walker, J. J.; Gutteridge, W. E., Screening of drugs for rapid activity against
684 Trypanosoma cruzi trypomastigotes in vitro. *Tropical medicine and parasitology : official organ*
685 *of Deutsche Tropenmedizinische Gesellschaft and of Deutsche Gesellschaft fur Technische*
686 *Zusammenarbeit* **1988,** *39* (2), 145-8; (c) Haido, R. M.; Esteves, M. J.; Barreto-Bergter, E.,
687 Amphotericin B-induced carbohydrate changes on the Trypanosoma cruzi surface membrane.
688 *The Journal of protozoology* **1992,** *39* (5), 609-12.
689 11. (a) Yardley, V.; Croft, S. L., In vitro and in vivo activity of amphotericin B-lipid
690 formulations against experimental Trypanosoma cruzi infections. *The American journal of*
691 *tropical medicine and hygiene* **1999,** *61* (2), 193-7; (b) Cencig, S.; Coltel, N.; Truyens, C.; Carlier,
692 Y., Parasitic loads in tissues of mice infected with Trypanosoma cruzi and treated with
693 AmBisome. *PLoS neglected tropical diseases* **2011,** *5* (6), e1216.
694 12. (a) Torrado, J. J.; Serrano, D. R.; Uchegbu, I. F., The oral delivery of amphotericin B.
695 *Therapeutic delivery* **2013,** *4* (1), 9-12; (b) Ching, M. S.; Raymond, K.; Bury, R. W.; Mashford, M.
696 L.; Morgan, D. J., Absorption of orally administered amphotericin B lozenges. *British journal of*
697 *clinical pharmacology* **1983,** *16* (1), 106-8.
698 13. Santangelo, R.; Paderu, P.; Delmas, G.; Chen, Z. W.; Mannino, R.; Zarif, L.; Perlin, D. S.,
699 Efficacy of oral cochleate-amphotericin B in a mouse model of systemic candidiasis.
700 *Antimicrobial agents and chemotherapy* **2000,** *44* (9), 2356-60.
701 14. Rassi, A., Jr.; Rassi, A.; Marin-Neto, J. A., Chagas disease. *Lancet* **2010,** *375* (9723), 1388-
702 402.
703 15. Sanchez-Brunete, J. A.; Dea, M. A.; Rama, S.; Bolas, F.; Alunda, J. M.; Raposo, R.; Mendez,
704 M. T.; Torrado-Santiago, S.; Torrado, J. J., Treatment of experimental visceral leishmaniasis with
705 amphotericin B in stable albumin microspheres. *Antimicrobial agents and chemotherapy* **2004,**
706 *48* (9), 3246-52.
707 16. Grossjohann, C.; Serrano, D. R.; Paluch, K. J.; O'Connell, P.; Vella-Zarb, L.; Manesiotis, P.;
708 McCabe, T.; Tajber, L.; Corrigan, O. I.; Healy, A. M., Polymorphism in sulfadimidine/4-
709 aminosalicylic acid cocrystals: solid-state characterization and physicochemical properties.
710 *Journal of pharmaceutical sciences* **2015,** *104* (4), 1385-98.
711 17. (a) British Pharmacopoeial Commission, British Pharmacopoeia, Appendix 1A; TSO:
712 Norwich, U.K. **2007,** *IV*, A61; (b) Lalatsa, A.; Lee, V.; Malkinson, J. P.; Zloh, M.; Schatzlein, A. G.;
713 Uchegbu, I. F., A prodrug nanoparticle approach for the oral delivery of a hydrophilic peptide,
714 leucine(5)-enkephalin, to the brain. *Molecular pharmaceutics* **2012,** *9* (6), 1665-80.
715 18. Al-Quadeib, B. T.; Radwan, M. A.; Siller, L.; Horrocks, B.; Wright, M. C., Stealth
716 Amphotericin B nanoparticles for oral drug delivery: In vitro optimization. *Saudi pharmaceutical*
717 *journal : SPJ : the official publication of the Saudi Pharmaceutical Society* **2015,** *23* (3), 290-302.
718 19. Espada, R.; Josa, J. M.; Valdespina, S.; Dea, M. A.; Ballesteros, M. P.; Alunda, J. M.;
719 Torrado, J. J., HPLC assay for determination of amphotericin B in biological samples. *Biomedical*
720 *chromatography : BMC* **2008,** *22* (4), 402-7.
721 20. Centers for disease control and prevention. Available from:
722 http://www.cdc.gov/dpdx/trypanosomiasisamerican/ Acesses date: 12/12/2016.
723 21. Romanha, A. J.; Castro, S. L.; Soeiro Mde, N.; Lannes-Vieira, J.; Ribeiro, I.; Talvani, A.;
724 Bourdin, B.; Blum, B.; Olivieri, B.; Zani, C.; Spadafora, C.; Chiari, E.; Chatelain, E.; Chaves, G.;
725 Calzada, J. E.; Bustamante, J. M.; Freitas-Junior, L. H.; Romero, L. I.; Bahia, M. T.; Lotrowska, M.;
726 Soares, M.; Andrade, S. G.; Armstrong, T.; Degrave, W.; Andrade Zde, A., In vitro and in vivo
727 experimental models for drug screening and development for Chagas disease. *Memorias do*
728 *Instituto Oswaldo Cruz* **2010,** *105* (2), 233-8.
729 22. Meirelles, M. N.; Chiari, E.; de Souza, W., Interaction of bloodstream, tissue culture-
730 derived and axenic culture-derived trypomastigotes of Trypanosoma cruzi with macrophages.
731 *Acta tropica* **1982,** *39* (3), 195-203.
732 23. Brener, Z., Therapeutic activity and criterion of cure on mice experimentally infected
733 with Trypanosoma cruzi. *Revista do Instituto de Medicina Tropical de Sao Paulo* **1962,** *4*, 389-96.

734 24. Gagos, M.; Arczewska, M., Spectroscopic studies of molecular organization of antibiotic
735 amphotericin B in monolayers and dipalmitoylphosphatidylcholine lipid multibilayers.
736 *Biochimica et biophysica acta* **2010,** *1798* (11), 2124-30.
737 25. Serrano, D. R.; Gallagher, K. H.; Healy, A. M., Emerging Nanonisation Technologies:
738 Tailoring Crystalline Versus Amorphous Nanomaterials. *Current topics in medicinal chemistry*
739 **2015,** *15* (22), 2327-40.
740 26. (a) Zu, Y.; Sun, W.; Zhao, X.; Wang, W.; Li, Y.; Ge, Y.; Liu, Y.; Wang, K., Preparation and
741 characterization of amorphous amphotericin B nanoparticles for oral administration through
742 liquid antisolvent precipitation. *European journal of pharmaceutical sciences : official journal of*
743 *the European Federation for Pharmaceutical Sciences* **2014,** *53*, 109-17; (b) Salerno, C.;
744 Chiappetta, D. A.; Arechavala, A.; Gorzalczany, S.; Scioscia, S. L.; Bregni, C., Lipid-based
745 microtubes for topical delivery of amphotericin B. *Colloids and surfaces. B, Biointerfaces* **2013,**
746 *107*, 160-6.
747 27. Jager, H. J.; Prinsloo, L. C., The dehydratation of phosphates monitored by DSC/TGA and
748 in situ Raman Spectroscopy. *Technochimica Acta* **2001,** *376*, 187-196.
749 28. Ono, M.; Anzai, H.; Tozuka, Y.; Moribe, K.; Oguchi, T.; Yamamoto, K., Water vapor
750 adsorption behavior of sodium deoxycholate anhydrous forms. *Chemical & pharmaceutical*
751 *bulletin* **2005,** *53* (2), 180-3.
752 29. Asher, I., Analitical Profiles of Drug Substances Academic Press London. **1977**.
753 30. Laniado-Laborin, R.; Cabrales-Vargas, M. N., Amphotericin B: side effects and toxicity.
754 *Revista iberoamericana de micologia* **2009,** *26* (4), 223-7.
755 31. (a) Italia, J. L.; Kumar, M. N.; Carter, K. C., Evaluating the potential of polyester
756 nanoparticles for per oral delivery of amphotericin B in treating visceral leishmaniasis. *Journal*
757 *of biomedical nanotechnology* **2012,** *8* (4), 695-702; (b) Wasan, K. M.; Sivak, O.; Bartlett, K.;
758 Wasan, E. K.; Gershkovich, P., Novel oral amphotericin B formulation (iCo-010) remains highly
759 effective against murine systemic candidiasis following exposure to tropical temperature. *Drug*
760 *development and industrial pharmacy* **2015,** *41* (9), 1425-30.
761 32. Vazquez, B. P.; Vazquez, T. P.; Miguel, C. B.; Rodrigues, W. F.; Mendes, M. T.; de Oliveira,
762 C. J.; Chica, J. E., Inflammatory responses and intestinal injury development during acute
763 Trypanosoma cruzi infection are associated with the parasite load. *Parasites & vectors* **2015,** *8*,
764 206.
765 33. Luna, K. P.; Hernandez, I. P.; Rueda, C. M.; Zorro, M. M.; Croft, S. L.; Escobar, P., In vitro
766 susceptibility of Trypanosoma cruzi strains from Santander, Colombia, to
767 hexadecylphosphocholine (miltefosine), nifurtimox and benznidazole. *Biomedica : revista del*
768 *Instituto Nacional de Salud* **2009,** *29* (3), 448-55.
769 34. Bellmann, R., Clinical pharmacokinetics of systemically administered antimycotics.
770 *Current clinical pharmacology* **2007,** *2* (1), 37-58.

771